# Structure of Gel Phase Saturated Lecithin Bilayers: Temperature and Chain Length Dependence

W.-J. Sun,* S. Tristram-Nagle,# R. M. Suter,* and J. F. Nagle*#
Departments of *Physics and #Biological Sciences, Carnegie Mellon University, Pittsburgh, Pennsylvania 15213 USA

ABSTRACT Systematic low-angle and wide-angle x-ray scattering studies have been performed on fully hydrated unoriented multilamellar vesicles of saturated lecithins with even chain lengths $N$ = 16, 18, 20, 22, and 24 as a function of temperature $T$ in the normal gel ($L_{\beta'}$) phase. For all $N$, the area per chain $A_c$ increases linearly with $T$ with an average slope $dA_c/dT$ = 0.027 Å$^2$/°C, and the lamellar $D$-spacings also increase linearly with an average slope $dD/dT$ = 0.040 Å/°C. At the same $T$, longer chain length lecithins have more densely packed chains, i.e., smaller $A_c$'s, than shorter chain lengths. The chain packing of longer chain lengths is found to be more distorted from hexagonal packing than that of smaller $N$, and the distortion $\epsilon$ of all $N$ approaches the same value at the respective transition temperatures. The thermal volume expansion of these lipids is accounted for by the expansion in the hydrocarbon chain region. Electron density profiles are constructed using four orders of low-angle lamellar peaks. These show that most of the increase in $D$ with increasing $T$ is due to thickening of the bilayers that is consistent with a decrease in tilt angle $\theta$ and with little change in water spacing with either $T$ or $N$. Because of the opposing effects of temperature on area per chain $A_c$ and tilt angle $\theta$, the area expansivity $\alpha_A$ is quite small. A qualitative theoretical model based on competing head and chain interactions accounts for our results.

## INTRODUCTION

The study of lipid bilayers has been and will continue to be greatly enriched by investigating how the structure and thermodynamic properties vary as the lipids are varied, including both naturally occurring and specifically synthesized lipids (Janiak et al., 1987; Lewis et al., 1987; Huang et al., 1994). One particularly appropriate strategy is to vary the chain length, because this variation systematically alters the balance between the interaction energy involving the headgroups, which remains the same, and the total interaction between the chains, which increases with chain length. As is well known, this variation yields increased main transition temperatures with increased chain length, but other structural changes, especially as a function of temperature, have not been so well documented.

Increasing chain length may involve dramatic changes. For example, for the phosphatidylethanolamines, decreasing chain length takes one from phase diagrams that have stable gel phases to phase diagrams in which the gel phase is merely metastable at all temperatures (Chang and Epand, 1983; Wilkinson and Nagle, 1984). In a recent study of a sequence of disaturated phosphatidylcholines from this laboratory, it was found that the wide-angle pattern in the gel phase started to become qualitatively different as the chain length $N$ was increased beyond 20 carbons (Tristram-Nagle et al., 1993), and various new phenomena have now been carefully documented by x-ray diffraction for $N$ = 24 (Sun et al., 1996) and by infrared spectroscopy for many chain lengths (Snyder et al., submitted for publication). Specifically, new gel-like phases appear, at both higher and lower temperatures. When these new phases are thoroughly understood, they will be valuable for what they can reveal about the competition between different forces that organize the gross structure of bilayers.

We have also been able to obtain and study the ordinary $L_{\beta'}$ gel phase for all chain lengths over extended temperature ranges. This kind of study, which is the subject of the present paper, is valuable for revealing the competition between different forces that organize the fine structure of the gel phase.

## MATERIALS AND METHODS

All lecithins were purchased in lyophilized form from Avanti Polar Lipids (1,2-dipalmitoyl-*sn*-glycero-3-phosphatidylcholine (to be abbreviated C16); 1,2-distearoyl-*sn*-glycero-3-phosphatidylcholine (C18); 1,2-diarachidoyl-*sn*-glycero-3-phosphatidylcholine (C20); 1,2-dibehenoyl-*sn*-glycero-3-phosphatidylcholine (C22); 1,2-dilignoceroyl-*sn*-glycero-3-phosphatidylcholine (C24)) and used without further purification. Oriented samples were prepared and analyzed as described by Tristram-Nagle et al. (1993).

Most of the work in this paper was on lipid/water dispersions, which were placed in 1 mm × 4 cm capillaries following standard procedures (Tristram-Nagle et al., 1993). Upon brief centrifugation, these dispersions separate into a lipid rich phase and a clear water rich phase, thus demonstrating full hydration. After scattering measurements, the lipid was assayed for radiation and thermal damage by thin-layer chromatography. The sample chamber holds a cassette with slots for 10 x-ray capillaries. The chamber is connected to a motorized 3D translational unit, which allows easy access of the x-ray beam to the capillaries and new spots on each capillary; this facilitates sample loading and allows us to minimize radiation damage by frequently translating unexposed sample into the beam. The temperature was controlled as described by Sun et al. (1996).

Our principle measurements were carried out using a rotating anode x-ray source interfaced with a four-circle diffractometer and a Braun linear position sensitive detector (PSD) as previously described (Sun et al., 1994). Accounting for the finite beam size, the finite sample size, and the diver-

*Received for publication 6 February 1996 and in final form 28 April 1996.*
Address reprint requests to Dr. John F. Nagle, Department of Physics, Carnegie Mellon University, 5000 Forbes Avenue, Pittsburgh, PA 15213. Tel.: 412-268-2764; Fax: 412-681-0648; E-mail: nagle@andrew.cmu.edu.

0006-3495/96/08/885/07 $2.00

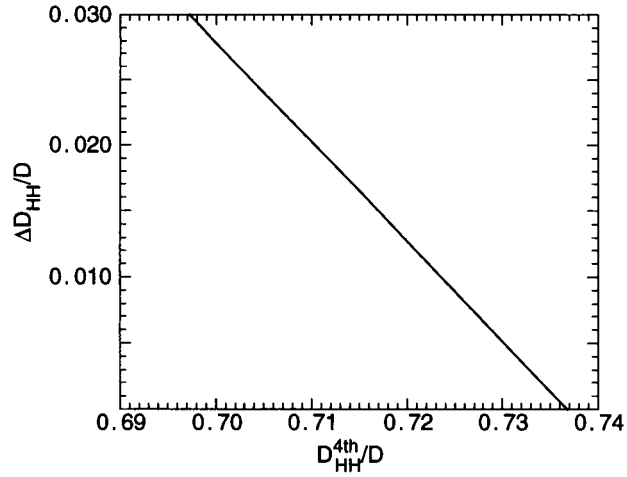


FIGURE 1 Corrections $\Delta D_{HH} = D^{4th}_{HH} - D^{true}_{HH}$, versus $D^{4th}_{HH}$, obtained from the electron density profile that was Fourier constructed using $h$ = 1–4 lamellar peaks for a known gel-phase electron density profile. Both axes are scaled by $1/D$ to account for all chain lengths and temperatures.

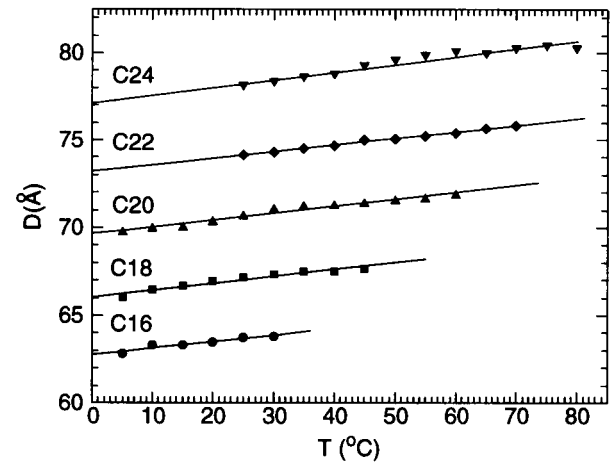


FIGURE 2 Lamellar $D$-spacing as a function of $T$ and $N$. Solid lines are linear least-square fits.

gence of the incoming beam leads to an estimate for the instrumental resolution of 0.065° (half-width half-maximum; HWHM) in $2\theta$ or $\Delta Q = 5 \times 10^{-3}$ Å$^{-1}$. The maximum exposure time on one spot was about 4 h with x-ray power of 5.25 kW, using a graphite monochromator. No radiation damage, as detected by changes in peak shapes, was detected in this time; thin-layer chromatography showed less than 1% lysolecithin for all of the samples.

Lamellar $D$ spacings were obtained quantitatively from the fourth-order peaks. This peak was well defined and was also less affected by slit smear than the lower order peaks. Taking into account slit smear, the lower order peaks indexed well with the fourth-order peak, except for C24 at low and high temperatures (Sun et al., 1996). Electron density profiles were obtained from the Lorentz-corrected intensities of the first four orders of low-angle diffraction in the usual way (Wiener et al., 1989).

Uncorrected head-head distances $D^{4th}_{HH}$ were obtained from the peak-peak distances in the fourth-order electron density profiles. We have found that $D^{4th}_{HH}$ is remarkably accurate, compared to larger and smaller numbers of Fourier components (Nagle et al., 1996). Nevertheless, we are interested in small differences as a function of temperature, so systematic corrections to $D_{HH}$ were estimated. We began with a known electron density profile of the one Gaussian hybrid type with parameters determined for the gel phase of C16 (Wiener et al., 1989). Later results in this paper (see Fig. 3) will show this correction to be applicable to other chain lengths. The fourth-order Fourier reconstruction from this model yielded values of $D^{4th}_{HH}$ for various values of $D^{true}_{HH}$. The relative error $(D^{4th}_{HH} - D^{true}_{HH})/D$ is plotted in Fig. 1 as a function of $D^{4th}_{HH}/D$, which can be obtained experimentally. Although the errors are fairly small, one sees that they vary systematically with the ratio $D^{4th}_{HH}/D$, which is the primary determinant for corrections. Fig. 1 was then used to obtain corrected values of $D_{HH}$ from experimental determinations of $D^{4th}_{HH}$ and $D$.

The orthorhombic lattice parameters for the chain packing, $a_c$ *and* $b_c$, were obtained using the standard formula

$$a_c = 2d_{20} \quad \text{and} \quad b_c = \frac{d_{11}}{\sqrt{1 - \left(\frac{d_{11}}{2d_{20}}\right)^2}}, \qquad (1)$$

where $d_{20}$ and $d_{11}$ are obtained using Bragg's law from the two wide-angle reflections.

## RESULTS AND DISCUSSION

### Low-angle scattering

Fig. 2 shows the interlamellar $D$ spacings. The $D$ spacings exhibit a smooth dependence upon both temperature $T$ and chain length $N$. The values of $D$ at 25°C and the slopes $dD/dT$ are reported in Table 1.

Fig. 3 shows the electron density profiles $\rho(z)$ along the bilayer normal for all chain lengths except C24, for which the low-angle data for the usual gel phase are too obscured by scattering from the new phases (Sun et al., 1996). The uncorrected head-head spacing $D^{4th}_{HH}$ is calculated as the distance between headgroup peaks in the same bilayer (from zero to around 50 Å) in Fig. 3. Results for $D_{HH}$ reported in Table 1 include systematic corrections to account for the

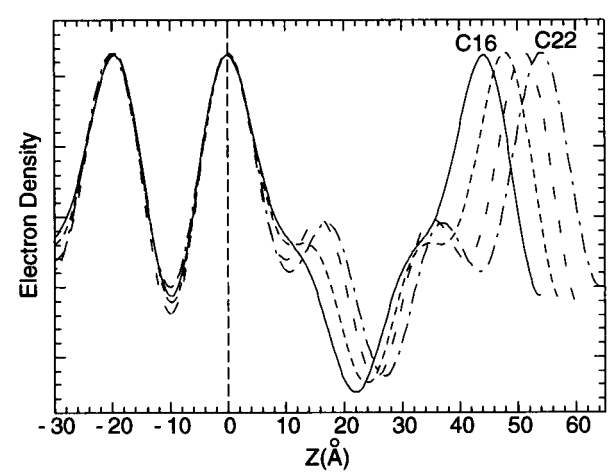


FIGURE 3 Electron density profiles at 25°C, Fourier constructed using $h$ = 1–4 peaks. Solid line, C16; short-dashed line, C18; long-dashed line, C20; dot-dashed line, C22. The heights of the headgroup peaks have been normalized to the same value. One headgroup peak has been placed at the origin for each chain length.

**TABLE 1 Values of structural quantities**

| $N$ | $D$ (Å) | $dD/dT$ (Å/°C) | $D_{HH}$ (Å) | $A_c$ (Å$^2$) | $dA_c/dT$ (Å$^2$/°C) | $dV_c/dT \times 10^4$ (ml/(g°C)) | $\theta$ (°) | $d\theta/dT$ (°/°C) | $A$ (Å$^2$) | $\alpha_A \times 10^4$ (°C$^{-1}$) |
|---|---|---|---|---|---|---|---|---|---|---|
| 16 | 63.8 | 0.037 (6) | 42.8 (2) | 20.2 (2) | 0.026 (3) | 9 (1) | 31.6 (4)[a]<br>31.6 (1)[b] | −0.10 (2) | 47.3 (3)<br>47.4 (4) | 2 (3) |
| 18 | 67.5 | 0.040 (4) | 47.0 (4) | 19.8 (1) | 0.029 (4) | 10 (1) | 32.5 (4)[a]<br>32.1 (1)[b] | −0.09 (1) | 47.3 (5)<br>46.8 (2) | 4 (3) |
| 20 | 71.0 | 0.039 (2) | 50.6 (3) | 19.6 (1) | 0.025 (3) | 9 (1) | 34.2 (4)[a]<br>33.6 (1)[b] | −0.08 (1) | 47.6 (2)<br>47.2 (2) | 3 (2) |
| 22 | 74.2 | 0.038 (2) | 53.9 (2) | 19.5 (1) | 0.027 (4) | 10 (1) | 35.7 (4)[a]<br>35.2 (1)[b] | −0.07 (1) | 47.6 (2)<br>47.8 (2) | 5 (2) |
| 24 | 78.1 | 0.044 (4) | 57.9 (3) | 19.3 (2) | 0.029 (3) | 11 (1) | 36.5 (4)[a]<br>35.4 (1)[b] | −0.07 (1) | 47.6 (4)<br>47.4 (4) | 6 (2) |

All values are for $T$ = 25°C.
[a]Measured on oriented films.
[b]Using Eq. 3 to obtain $\theta$, except for C16.

effects of Fourier truncation as described in Materials and Methods. In this paper we will define the water spacing $D_W$ to be the distance between headgroup peaks on adjacent bilayers (from zero to about −20 Å in Fig. 3), so $D_W = D - D_{HH}$. This definition of $D_W$ overestimates the space that is exclusively occupied by water, because the lipid heads obviously extend some 4–5 Å beyond the headgroup peaks, and one would wish to subtract 8–10 Å from our $D_W$ to discuss interbilayer forces (McIntosh and Simon, 1986; McIntosh et al., 1989). McIntosh and Simon (1986) reported a fluid layer thickness of 11.7 Å for fully hydrated C16 at 20°C; using their definition for the fluid layer thickness, which is $D_W$ − 10 Å, we obtain a fluid layer thickness of 11.0 Å for fully hydrated C16 at 25°C.

Fig. 4 shows $D_{HH}/2$ and $D_W$ as a function of temperature for four chain lengths. As would be expected, the thickness of the bilayers $D_{HH}$ systematically increases as the chain length increases. In contrast, the water spacing is nearly the same for all chain lengths. From the results in Fig. 4, the slope $dD_{HH}/dT$ is at least 5 times greater than the slope $dD_W/dT$, so most of the thermal increase in $D$ is due to thickening of the bilayer rather than to thickening of the water layer. It may be noted that our Fourier truncation corrections only increase $dD_{HH}/dT$ by a factor of 1.1. Simon et al. (1995) obtained values of $D_{HH}$ for C22 at 23°C and 50°C that agree with ours within 0.1 Å, although the temperature dependence of their water spacing ($dD_W/dT$) was about twice as large as ours before we applied our correction. Our result that the water thickness is nearly independent of temperature and chain length has previously been obtained by Kirchner and Cevc (1994), although their values for $dD/dT$ and other quantities to be discussed differ somewhat from those in Table 1.

## Wide-angle scattering

For the ordinary $L_{\beta'}$ gel phase, wide-angle scattering shows the usual sharp (20) peak and a broad (11) peak for all chain

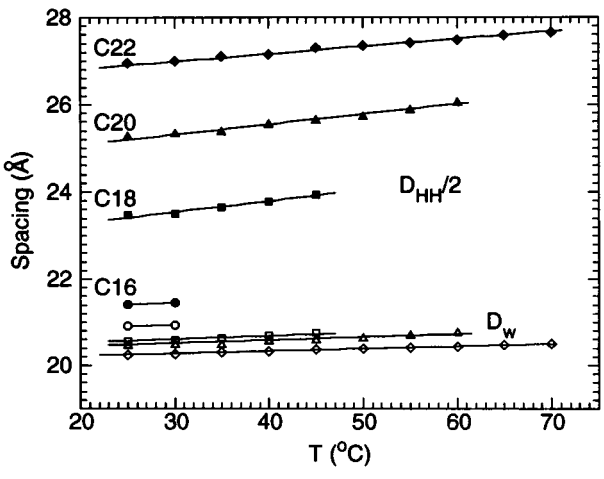


FIGURE 4 Corrected $D_{HH}/2$ (solid symbols) and $D_W$ (open symbols) as a function of temperature. Circles, C16; squares, C18; triangles, C20; diamonds, C22. Lines are linear least-square fits.

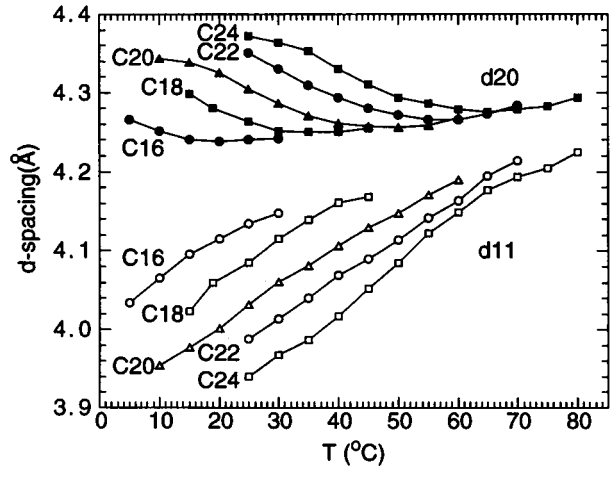


FIGURE 5 Temperature and chain length dependence of the wide-angle $d_{11}$ (open symbols) and $d_{20}$ (closed symbols) in Å. Circles, C16; squares, C18; triangles, C20; diamonds, C22; inverted triangles, C24. Lines are to guide the eye.

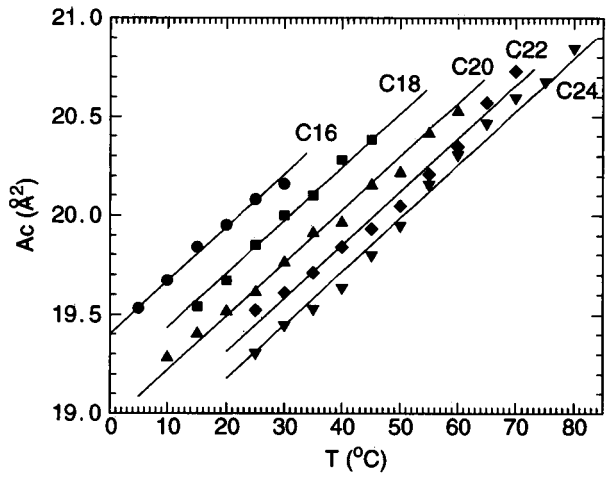


FIGURE 6 Temperature and chain length dependence of the area per chain, $A_c$. Solid lines are linear least-square fits with the slopes fixed to the averaged value (0.027 Å²/°C) of all chains lengths.

lengths $N$. As has been known for a long time, these peaks indicate orthorhombic packing of nearly all-*trans* hydrocarbon chains tilted toward nearest neighbors (Sun et al., 1994; Levine, 1970; McIntosh, 1980). Fig. 5 shows the temperature and chain length dependence of the $d$ spacings from the two wide-angle peaks. As $N$ increases, the curves are displaced to higher temperatures, but retain their shape as a function of $T$.

The area per chain in the plane perpendicular to the chains, $A_c$, is calculated from $d_{20}$ and $d_{11}$, assuming orthorhombic packing with two chains per unit cell, using the formula $2A_c = a_c b_c$, and Eq. 1 for $a_c$ and $b_c$. As expected, the chains are packed more tightly at lower temperatures, so $A_c$ expands with temperature, as shown in Fig. 6. Assuming that the chains are in nearly all-*trans* conformations, the volume $V_c$ of the hydrocarbon chain region is given by $V_c = 2N(1.27\ \text{Å})A_c$, where 1.27 Å is the distance between adjacent methylenes projected onto the chain axis. The wide-angle data therefore yield the hydrocarbon volume expansion coefficients $dV_c/dT$ shown in Table 1. For the volume $V_L$ of the entire lipid, dilatometry (Nagle and Wilkinson, 1978) has given $dV_L/dT = 8.3(5) \times 10^{-4}$ml/g°C for C16 and C18. Within error, $dV_L/dT$ and $dV_c/dT$ are the same, indicating that thermal changes in lipid volume are accounted for by the hydrocarbon chain region, as originally suggested by Nagle and Wilkinson (1978) from much less extensive x-ray data. It may also be noted that the sign of the small differences would require a small volume shrinkage of the headgroup and glycerol parts of the lipid bilayer with increasing temperature.

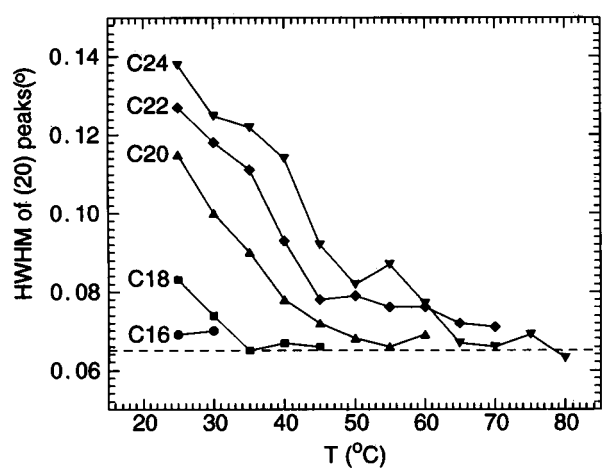


FIGURE 7 Temperature and chain length dependence of the half-width at half maximum (HWHM) of the (20) peaks (in degrees). The dashed line shows the instrumental resolution.

The widths of the sharp (20) wide-angle peaks, shown in Fig. 7, decrease with increasing temperature. The leveling out of the apparent half-widths at the higher temperatures is an artifact of the instrumental resolution of about 0.065° (HWHM), as shown in Fig. 7. A higher resolution study (Sun et al., 1994) obtains 0.015° (HWHM) for the intrinsic half-width of the (20) peak for C16 at 25°C. Because the intrinsic half-width of the (20) peak is usually inversely proportional to the correlation length of the chain packing order, it is surprising that the half-width decreases with increasing temperature, because one would expect the sample to become more disordered with smaller correlation lengths at higher temperatures. It is also remarkable that longer chain lipids with stronger cohesive van der Waals forces between chains should have shorter correlation lengths. Our temperature reversibility study on C24 (Sun et al., 1996) showed that the HWHM result in Fig. 7 was reproducible as the temperature was raised and lowered, so the temperature dependence in Fig. 7 is not due to gradual annealing as the samples are warmed. We also note that the much wider (11) peak width is expected to decrease with increasing temperature because the chain tilt decreases and the (11) peak is off the equator in $q$-space, but that this explanation does not apply to the (20) peak because it is on the equator (Sun et al., 1994).

Fig. 5 also shows that as temperature increases, $d_{20} - d_{11}$ decreases, which means that the chain packing moves toward hexagonal, for which $d_{20} = d_{11}$. A principle reason that the chain packing is not hexagonal is that hydrocarbon chains are not simple cylinders. Sirota et al. (1993) have identified an appropriate measure of the orthorhombic distortion from hexagonal packing, namely the distortion order parameter, defined as

$$\epsilon = 1 - \frac{a_c}{\sqrt{3}b_c}, \qquad (2)$$

where $a_c$ and $b_c$ are the orthorhombic lattice parameters defined in Eq. 1. The magnitude of $\epsilon$ measures the amount of distortion, and the sign shows the direction of the distortion; a negative sign means stretching along $a_c$, and a positive sign means stretching along $b_c$. Our results for $\epsilon$ are plotted in Fig. 8. For each chain length $N$, the magnitude of the distortion $|\epsilon|$ decreases with increasing temperature;

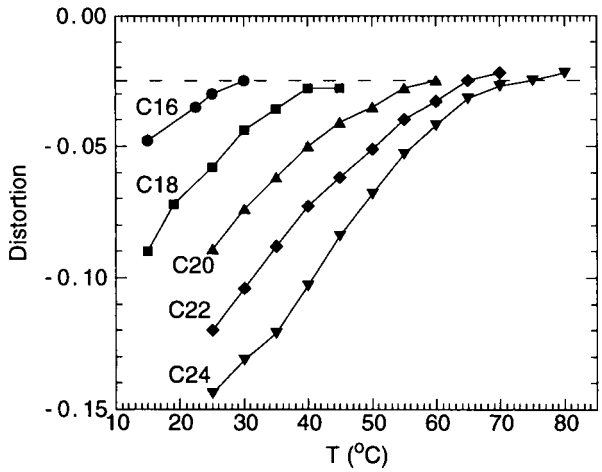


FIGURE 8 Temperature and chain-length dependence of the distortion parameter $\epsilon$ (defined in Eq. 2).

similar results have also been reported by Sirota et al. (1993) for long-chain alkanes. This can be understood because the noncylindrical steric forces between hydrocarbon chains are relatively stronger at closer packing (smaller $A_c$) at lower temperatures than at higher temperatures, where the attractive van der Waals interaction, which is more cylindrically symmetric, plays a relatively larger role. We find it especially intriguing that the lipids of all chain lengths undergo a transition out of the gel phase when the magnitude of the distortion decreases to about 0.025, as seen in Fig. 8. We know of no fundamental theory that has predicted this. This result looks like a clue for understanding gel phase stability, but one must remember that the transition out of the gel phase is a first-order transition, so the thermal behavior of the higher temperature phase, which is a ripple phase for lower values of $N$ and is thought to be an $L_\alpha$ phase for C24 (Lewis et al., 1987), should also play a role.

## Tilt angle $\theta$

The tilt angle $\theta$ of the hydrocarbon chains in the $L_{\beta'}$ phase has been measured directly on fully hydrated oriented films in this and previous work (Tristram-Nagle et al., 1993). For C16 it has also been possible to obtain the tilt angle in unoriented MLV powder samples (Sun et al., 1994) like those employed here, and the value $\theta = 31.6°$ obtained at 25°C agrees with our results from oriented samples. Measured values of $\theta$ from oriented films at or near 25°C are shown by the first entry under $\theta$ in Table 1 with superscript *a*. For the temperature dependence of $\theta$, Fig. 9 shows data for an oriented C16 sample taken over a larger temperature range. Although it is the subgel phase rather than the gel phase that is thermodynamically stable at the lower three temperatures in Fig. 9, the subgel phase does not form in C16 unless the temperature is decreased below 7°C for a long enough time to incubate it (Nagle and Wilkinson, 1982). The wide- and low-angle patterns confirmed that our oriented samples were in the gel phase at all temperatures in Fig. 9. Fig. 9 gives a best fitted value $d\theta/dT = -0.16°/°C$. Furthermore, there is no doubt that $d\theta/dT$ is negative (Janiak et al., 1976; Kirchner and Cevc, 1994); the least temperature-dependent value that can be justified from Fig. 9 is $d\theta/dT = -0.10°/°C$. This latter value is close to the value of $-0.11°/°C$ for C16 that we estimate from the $\theta$ versus $T$ data that Janiak et al. (1976) obtained using the gravimetric method.

In this paragraph we shall analyze our low-angle data to obtain an indirect determination of $d\theta/dT$ for all chain lengths. From Fig 4 we find that $dD_{HH}/dT$ is practically the same as $dD/dT$ shown in Table 1. Assuming that the change in $D_{HH}$ is due to changes in chain tilting, then

$$D_{HH} = 2N(1.27\ \text{Å})\cos\theta + 2D_H, \quad (3)$$

where $2D_H$ accounts for the headgroup thickness, which is assumed not to change with temperature. Then,

$$dD_{HH}/dT = -2N(1.27\ \text{Å})(\sin\theta)(d\theta/dT). \quad (4)$$

The values of $d\theta/dT$ calculated from Eq. 4 are shown in Table 1.

Although the value of $d\theta/dT$ obtained in the preceding paragraph is consistent with the extreme upper end of the range for $d\theta/dT$ obtained from our direct measurements of C16, we are concerned with the possible discrepancy, and so we have considered possible changes in the model that might bring them into better agreement. However, all of the most plausible changes we have thought of, such as the one in the last paragraph of this subsection, make the disagreement worse. The best model we can derive that changes our calculated value shown in Table 1 to our best measured value of $-0.16°/°C$ would require that the headgroup thickness $D_H$ decrease with increasing temperature.

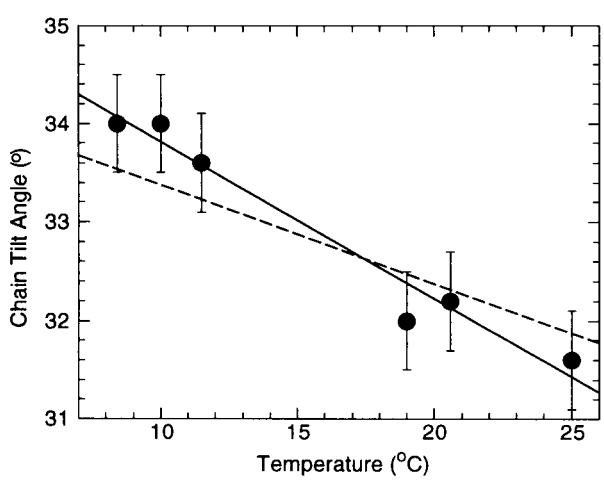


FIGURE 9 Temperature dependence of the tilt angle $\theta$ of C16 obtained from oriented samples. The solid line is the best linear least-square fit to the data, with $d\theta/dT = -0.16°/°C$; the dashed line has $d\theta/dT = -0.10°/°C$.

In this paragraph let us turn from temperature dependence to chain length dependence. Our best established tilt angle is $\theta = 31.6°$ for C16 at 25°C. Together with $D_{HH}$ from Fig. 4, Eq. 3 yields $D_H = 4.12$ Å. Using this value of $D_H$ for other chain lengths yields the second set of $\theta$ values in Table 1 with the superscript *b*. Agreement with directly measured tilt angles (indicated by superscript *a*) is satisfactory.

Another model that has been considered by Kirchner and Cevc (1994) assumes that the heads are tilted with the same angle as the chains. In place of Eq. 3 one then has

$$D_{HH} = (2N(1.27\ \text{Å}) + 2D_H)\cos\theta. \quad (5)$$

Following the same procedures as in the preceding paragraph, we obtain, for $N = 18$, 20, 22, and 24, $\theta = 31.8°$, 33.1°, 34.6°, and 34.9°, respectively, using Eq. 5. Because these are in poorer agreement with our direct measurements of $\theta$, we suggest that the effective tilt of the headgroups is not rigidly coupled to the tilt of the chains and that Eq. 3 is superior to Eq. 5. Using Eq. 5, Kirchner and Cevc (1994) obtained a $d\theta/dT$ of about $-0.18°/°C$. The sign of their result concurs with our earlier (Tristram-Nagle et al., 1993) and present study, but the absolute value, which would be even larger if Eq. 4 were used, is about twice as large as our values presented in Table 1.

### Interfacial area *A*

The area $A$ that each lipid occupies on average at the interface with the water space is given by

$$A = 2A_c/\cos\theta. \quad (6)$$

Table 1 shows two sets of values of $A$ for $T = 25°C$ obtained using our two determinations of $\theta$. As was emphasized in our early work (Tristram-Nagle et al., 1993), $A$ is nearly constant as a function of chain length.

The temperature dependence of $A$ is obtained by differentiating Eq. 6. Then, the area expansivity defined by $\alpha_A = (dA/dT)/A$ is given by

$$\alpha_A = [(dA_c/dT)/A_c] + [(\tan\theta)(d\theta/dT)]. \quad (7)$$

Values of $\alpha_A$ calculated using our data and Eq. 7 are shown in Table 1. The most remarkable result is how small $\alpha_A$ is for all chain lengths. Even for a 50°C increase in $T$, $A$ would only increase by 1.4 Å$^2$ for C24. A significant reason for small $\alpha_A$ is the competition of thermal expansion of the chain packing and of the chain tilting. As would be expected, the chain lattice expands thermally, so that the first term in Eq. 7, $[(dA_c/dT)/A_c]$, is positive. However, the second term in Eq. 7 is negative because chain tilt decreases with increasing temperature. Because the magnitudes (about 0.001/°C) of the two nearly equal terms are comparable, the magnitude of $\alpha_A$ is smaller than one would obtain from either term alone. Furthermore, this cancellation of terms, each of which has errors, suggests that the fairly large relative increase of $\alpha_A$ with $N$ seen in Table 1 may not be significant. In this regard, it is worth noting that, for C16, our direct measurements of $d\theta/dT = -0.16°/°C$ would even yield negative values for $\alpha_A$.

Values of $\alpha_A$ from $+5 \times 10^{-4}$ (Evans and Kwok, 1982) to $+3 \times 10^{-3}$ (Needham and Evans, 1988) have been reported from studies of giant unilamellar vesicles of C14. It is quite impossible that our multilamellar vesicles could have values of $\alpha_A$ greater than $1.5 \times 10^{-3}/°C$, because this number comes from the first term in Eq. 7 determined directly from our wide-angle results for $A_c$, and the effect of tilt angle in the last term in Eq. 7 only decreases $\alpha_A$. Although one might wish to consider that $\alpha_A$ might be different for gel phases in giant unilamellar versus multilamellar vesicles or for C14 versus longer chain lengths, these papers emphasize that obtaining results for the gel phase of giant unilamellar vesicles is much more problematical than for the higher temperature phases.

Dynamical light scattering data on small unilamellar vesicles led Kirchner and Cevc (1994) to conclude that $\alpha_A$ is negative, and they then based a new theory of the pretransition on this conclusion. They argued that this conclusion was plausible because the tilt angle decreases with increasing temperature. Their argument, however, neglected the increase in the chain packing area $A_c$ with increasing temperature, which adds a positive term to $\alpha_A$, as shown in Eq. 7, and compensates for the negative contribution to $\alpha_A$ from the decreasing chain tilt.

## THEORETICAL INTERPRETATION

In our earlier paper (Tristram-Nagle et al., 1993) we had shown that the area $A$ and the water region were nearly independent of chain length. We advanced a theory for this that will apply equally well to our new results that the area $A$ and the water region are also nearly independent of temperature, whereas the thickness $D_{HH}$ of the bilayer and the chain tilt angle $\theta$ have significant temperature variations. That theory is based on the explanation (Nagle, 1976; McIntosh, 1980) that chains tilt because of competing interactions in the head and chain regions of the lipid molecule. Specifically, there is a strong steric repulsive interaction between headgroups for areas $A$ less than 48 Å$^2$ (Tristram-Nagle et al., 1993). However, the natural area $2A_c$ for the packing of all-*trans* hydrocarbon chains is only about 40 Å$^2$. To minimize the total energy due to both headgroup and chain interactions, the chains tilt at an angle $\theta$, so that both the heads and the chains can fit into the geometric constraint of a flat bilayer. However, there is still competition between heads and chains because the chains, by themselves, would prefer not to tilt as much as is required by the steric interaction of the heads. The chains then exert a pressure on the headgroups that pushes them together, so that they are in the strongly repulsive, and therefore less elastic, portion of the head-head interaction energy function. Therefore, the area $A$ changes little as the external forces on the heads change, e.g., because of changes in chain length or temperature. However, the chains are in the much more elastic, and

probably attractive, portion of the chain-chain interaction energy function. As the temperature rises, the chain packing area $A_c$ naturally increases significantly. This allows the chain tilt to decrease, while keeping the headgroup spacing nearly constant on the less elastic portion of the head-head interaction energy function.

Our result that the water spacing $D_W$ in the gel phase does not depend significantly upon temperature is also understandable if the interbilayer forces do not depend much upon temperature. Recently, Simon et al. (1995) showed that the principal repulsive force in the gel phase of C22 is the hydration force and that it is nearly independent of temperature. The other principal interbilayer force is the van der Waals force (Israelachvili, 1985), which is essentially given as

$$F_W = -\frac{W}{6\pi}\left[\frac{1}{d_W^3} - \frac{2}{(D_W + D_{HH})^3} + \frac{1}{(D_W + D_{HH})^3}\right]. \quad (8)$$

Although the magnitude of the van der Waals force should become larger with increasing temperature because of changing $D_{HH}$, the increase due to that change is less than 0.5% over a temperature interval of 45°C using our measured changes in $D_{HH}$.

We therefore conclude that the major thermal changes in lecithin bilayers within the usual $L_{\beta'}$ thermodynamic phase are changes in chain packing area $A_c$ and in tilt angle $\theta$. Because the headgroups are always packed together very strongly, much smaller changes occur in the headgroup area. Because the lipid/water interface does not change, it is then not surprising that the water spacing does not change much with temperature or with chain length.

This research was supported by NIH grant GM44976.

## REFERENCES


Chang, H., and R. M. Epand. 1983. The existence of a highly ordered phase in fully hydrated dilauroylphosphatidylethanolamine. *Biochim. Biophys. Acta.* 728:319–324.

Evans, E. A., and R. Kwok. 1982. Mechanical calorimetry of large DMPC vesicles in the phase transition region. *Biochemistry.* 21:4874–4879.

Huang, C. Z. Wang, H. Lin, E. E. Brumbaugh, and S. Li. 1994. Interconversion of bilayer phase transition temperatures between phosphatidylethanolamines and phosphatidylcholines. *Biochim. Biophys. Acta.* 1189:7–12.

Israelachvili, J. N. 1985. Intermolecular and Surface Forces. Academic Press, London.

Janiak, M. J., D. M. Small, and G. G. Shipley. 1976. Nature of the thermal pretransition of synthetic phospholipids: dimyristoyl- and dipalmitoyllecithin. *Biochemistry.* 15:4575–4580.

Kirchner, S., and G. Cevc. 1994. On the origin of thermal $L_{\beta'}$ to $P_{\beta'}$ pretransition in the lamellar phospholipid membranes. *Europhys. Lett.* 28:31–36.

Levine, Y. K. 1970. X-ray diffraction studies of membranes. Ph.D. thesis. University of London.

Lewis, R. A. N. H., N. Mak, and R. N. McElhaney. 1987. A differential scanning calorimetric study of the thermotropic phase behavior of model membranes composed of phosphatidylcholines containing linear saturated fatty acyl chains. *Biochemistry.* 26:6118–6126.

McIntosh, T. J. 1980. Difference in hydrocarbon chain tilt between hydrated PEs and PCs. *Biophys. J.* 29:237–245.

McIntosh, T., A. D. Magid, and S. A. Simon. 1989. Hydration force in bilayer systems. *Biochemistry.* 28:17–25.

McIntosh, T. J., and S. A. Simon. 1986. Hydration force and bilayer deformation: a reevaluation. *Biochemistry.* 25:4058–4066.

Nagle, J. F. 1976. Theory of lipid monolayer and bilayer phase transition: effect of headgroup interactions. *J. Membr. Biol.* 27:233–250.

Nagle, J. F., and D. A. Wilkinson. 1978. Lecithin bilayers: density measurements and molecular interactions. *Biophys. J.* 23:159–175.

Nagle, J. F., and D. A. Wilkinson. 1982. Dilatometric studies of the subtransition in DPPC. *Biochemistry.* 21:3817–3821.

Nagle, J. F., R. Zhang, S. Tristram-Nagle, W.-J. Sun, H. Petrache, and R. M. Suter. 1996. X-ray structure determination of fully hydrated $L_\alpha$ phase DPPC bilayers. *Biophys. J.* 70:1419–1431.

Needham, D., and E. A. Evans. 1988. Structure and mechanical properties of giant lipid vesicle bilayers from 20°C below to 10°C above the liquid crystal-crystalline phase transition at 24°C. *Biochemistry.* 21: 8261–8269.

Simon, S. A., S. Advani, and T. J. McIntosh. 1995. Temperature dependence of the repulsive pressure between phosphatidylcholine bilayers. *Biophys. J.* 69:1473–1483.

Sirota, E. B., H. E. King, D. M. Singer, and H. H. Shao. 1993. Rotator phases of the normal alkanes: an x-ray scattering study. *J. Chem. Phys.* 98:5809–5824.

Snyder, R. G., G. L. Liang, and H. L. Strauss. 1996. Phases and phase behavior of long-chain dialkylphosphatidylcholine gels via infrared spectroscopy. *Biophys. J.* In press.

Sun, W.-J., R. M. Suter, M. A. Knewtson, C. R. Worthington, S. Tristram-Nagle, R. Zhang, and J. F. Nagle. 1994. Order and disorder in fully hydrated unoriented bilayers of gel phase DPPC. *Phys. Rev. E.* 49: 4665–4676.

Sun, W.-J., S. Tristram-Nagle, R. M. Suter, and J. F. Nagle. 1996. Anomalous phase behavior of long chain saturated lecithin bilayers. *Biochim. Biophys. Acta.* 1279:17–24.

Tristram-Nagle, S., R. Zhang, R. M. Suter, C. R. Worthington, W.-J. Sun, and J. F. Nagle. 1993. Measurement of chain tilt angle in fully hydrated bilayers of gel phase lecithins. *Biophys. J.* 64:1097–1109.

Wiener, M. C., R. M. Suter, and J. F. Nagle. 1989. Structure of the fully hydrated gel phase of DPPC. *Biophys. J.* 55:315–325.

Wilkinson, D. A., and J. F. Nagle. 1984. Metastability and the subtransition in phosphatidylethanolamine bilayers. *Biochemistry.* 23:1538–1541.